A hybrid silicon evanescent electroabsorption modulator

Ying-hao Kuo, Hui-wen Chen, and John E. Bowers
Department of Electrical and Computer Engineering, University of California Santa Barbara, Santa Barbara, CA 93106
yinghao.kuo@ece.ucsb.edu

Abstract: A new way to make high speed modulators using Si waveguides is demonstrated. The hybrid silicon evanescent electroabsorption modulator with offset AlGaInAs quantum wells has an extinction ratio over 10dB and modulation bandwidth over 16GHz.
©2007 Optical Society of America
OCIS codes: (250.4410) Modulators; (250.5300) Photonic integrated circuits; (250.7360) Waveguide modulators.

1. Introduction

Silicon-based modulators have attracted much attention with devices reported using the free carrier plasma dispersion in Mach-Zehnder interferometric form [1,2] or with resonator structure [3,4] to increase the interaction of light with the active material. Strained silicon also exhibits linear electro-optic refractive index modulation [5]. Recently electroabsorption modulator on silicon had been demonstrated based on the Franz-Keldysh effect in strained SiGe [6]. Here we present our approach of integration of modulators into silicon using wafer bonded hybrid silicon evanescent platform. The modulator described here can be integrated with lasers [7], amplifiers, and photodetectors [8] using quantum well intermixing [9]. High performance integrated high speed transmitters should be possible.

2. Device structure and fabrication

The silicon evanescent electroabsorption modulator (EAM) is a hybrid structure that consists of an offset multiple quantum well (MQW) region bonded to a silicon waveguide fabricated on a silicon-on-insulator (SOI) wafer as shown in Fig. 1. The III-V epitaxial structure is grown on an InP substrate. The structure is summarized in Table 1. InGaAlAs is chosen as the MQW material because it has larger ΔE_c, which provides a stronger carrier confinement and produce strong quantum confined stark effect (QCSE) with higher extinction ratio [10,11]. The MQW section contains 10 wells and 11 barriers with photoluminance (PL) at 1478nm. The silicon waveguide was fabricated with a height of 0.5μm and slab thickness of 0.3μm. The silicon waveguide has a width of 1.5μm for passive segments, and width of 0.8um under III-V mesa for higher optical confinement. The width of the III-V mesa for the absorber is 4μm at the top InP cladding layer and 2μm at the SCH and MQW layers to reduce the capacitance of the device [11,12]. Figure 1b shows the transition between the passive silicon waveguide and the hybrid waveguide of the EAM. The width of the III-V mesa is tapered from 0 to 2μm over a length of 60μm to increase the coupling efficiency and to minimize reflection. The center of the absorption region is kept with width of 4μm to avoid laterally affect the optical mode and reduce the voltage drop at InP cladding. The contact electrode pads are designed to be 100μm apart from center to center to use a standard GSG RF probe for high speed testing. The hybrid device has a total length around 400μm with 100μm absorber and two 60μm long tapers.

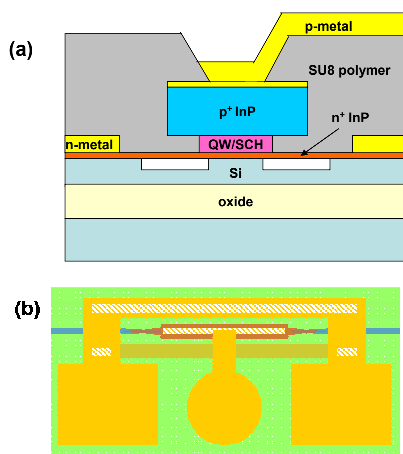

Fig. 1. Schematic diagrams of (a) device cross section and (b) hybrid waveguide and metal contacts.

	Layer	Material and Composition	Doping	Thickness
1	P Contact	$In_{0.53}Ga_{0.47}As$	P – 1e19	0.1 μm
2	Cladding	InP	P – 1e18	1.5 μm
3	SCH	$In_{0.520}Al_{0.160}Ga_{0.320}As$, -0.06%, 1.30 μm	P – 1e17	0.15 μm
4	MQW (λ_{PL}~1.48 μm)	$In_{0.590}Al_{0.080}Ga_{0.330}As$, +0.41%, 1.55 μm (10x)	n. i. d.	11 nm
		$In_{0.470}Al_{0.200}Ga_{0.330}As$, -0.40%, 1.19 μm (11x)	n. i. d.	7 nm
5	SCH	$In_{0.520}Al_{0.160}Ga_{0.320}As$, -0.06%, 1.30 μm	n. i. d.	0.1 μm
6	N Contact	InP	N – 3e18	0.11 μm
7	Super lattice	$In_{0.85}Ga_{0.15}As_{0.327}P_{0.673}$ (2x)	N – 3e18	7.5 nm
		InP (2x)	N – 3e18	7.5 nm
8	Bonding layer	InP	N – 3e18	10 nm

Table 1. III-V epitaxial layer structure.

The III-V epitaxial layers are transferred to the patterned SOI wafer through low temperature oxygen plasma assisted wafer bonding at a 300 ºC annealing temperature under vacuum. The InP substrate is removed using a mixture of HCl/H_2O. The details of silicon waveguide fabrication and wafer bonding process are described in Ref. 7. The III-V back end processing starts with blanket deposition of Pd/Ti/Pd/Au p-contacts. The p metal serves as a hard mask for the self aligned process to form the III-V mesa [8]. The undercut profile is created by wet etch SCH and MQW layers. Ni/Au/Ge/Ni/Au alloy are deposited onto the exposed n-type InP layer to form ohmic contacts. The n-InP layer is selectively removed by RIE dry etch to expose the silicon input and output waveguides. A 4µm thick SU-8 polymer layer is used to minimize the parasitic capacitance between the p-probe pad and the n-type InP layer and to provide additional mechanical support to the thin n-InP layer over the silicon waveguide air gap. 2 µm Ti/Au probe pads are deposited and connected to contact metals for final electrical contact.

3. Device characteristics

Figure 2 shows the relative extinction at wavelength of 1550nm under various reverse biases. More than 10dB extinction can be achieved with 5V bias. The device has a series resistance around 30Ω and capacitance of 0.1pF measured from impedance test, which will results a cut-off frequency around 20GHz. It matches with the measured small signal modulation response as shown in Fig. 3.

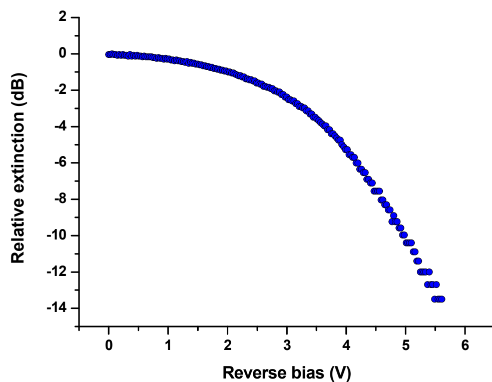

Fig. 2. Relative optical extinction at different DC bias.

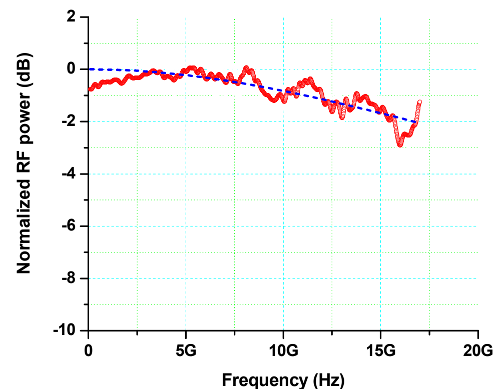

Fig. 3. Small signal response. Dashed line: calculated response using RC model.

To investigate the performance of large signal modulation, we drive our modulator with a 2^{31}-1 pseudorandom bit sequence (PRBS). The device is biased at -3V with peak to peak drive voltage of 3.2V. The modulated light is collected with lensed fiber and amplified with EDFA. A 100GHz filter is used to reduce the ASE noise before the signal is detected by a 30GHz photodetector and sampled using an Agilent digital communication analyzer (DCA). Figure 4a shows eye diagrams measured at non-return-to-zero (NRZ) 10 Gb/s. The 10 Gb/s signal has an extinction ratio of 6.3 dB, which is slightly lower than the DC extinction due to microwave voltage drop at cladding and ohmic contacts. The eye is clearly open with quality factor (Q factor) close to 12. The rise and fall time of the signal is about 27ps, which is as expected faster than the driving signal as shown in Fig. 4b.

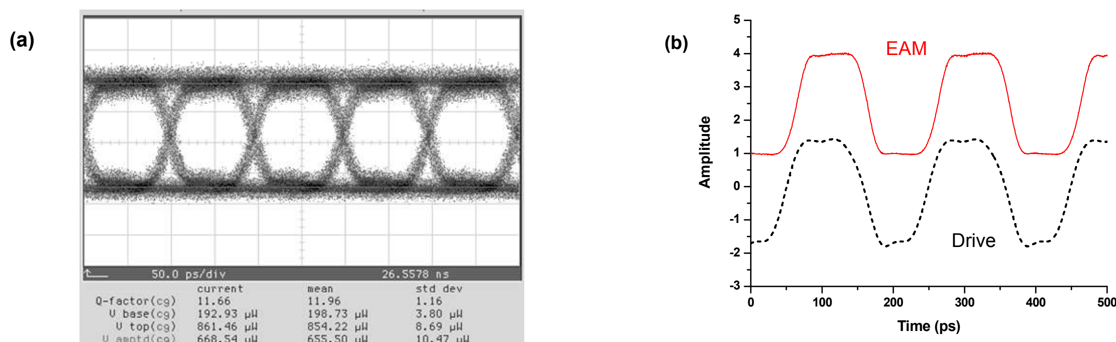

Fig. 4. (a) Measured 10G NRZ eye diagrams; (b) pulse train of drive signal and modulated signal. The drive signal has rise/fall time around 35ps. The modulated signal shows better rising/falling edge about 27ps.

OThC1.pdf

4. Conclusion

We have demonstrated the first hybrid silicon evanescent electroabsorption modulator with offset AlGaInAs quantum well. The fabricated device has DC extinction ratio over 10dB at 5V bias. The small signal modulation bandwidth is over 16G Hz. We presented a clear eye opening at 10Gb/s with peak to peak drive voltage of 3.2V. The current device is RC limited to 20Ghz bandwidth. By employing travel wave electrode with longer absorber, we can further improve the bandwidth and extinction ratio. The approach developed here is not limited by the relatively weak, relatively slow response of carrier injection Si modulators.

The authors acknowledge financial support from DARPA and the Army through contract W911NF-05-1-0175

5. References

[1] A. S. Liu, R. Jones, L. Liao, D. Samara-Rubio, D. Rubin, O. Cohen, R. Nicolaescu, and M. Paniccia, “A high-speed silicon optical modulator based on a metal-oxide semiconductor capacitor,” *Nature* **427**, 615–-618 (2004).

[2] D. Marris-Morini, X. Le Roux, L. Vivien, E. Cassan, D. Pascal, M. Halbwax, S. Maine, S. Laval, J. M. Fedeli, and J. F. Damlencourt, “Optical modulation by carrier depletion in a silicon PIN diode,” *Opt. Express* **14**, 10838-10843 (2006).

[3] Y. Q. Jiang, W. Jiang, L. L. Gu, X. N. Chen, and R. T. Chen, “80-micron interaction length silicon photonic crystal waveguide modulator,” *Appl. Phys. Lett.* **87**, 221105-1-3 (2005).

[4] Q. Xu, B. Schmidt, S. Pradhan, and M. Lipson, “Micrometre-scale silicon electrooptic modulator,” *Nature* **435**, 325-327 (2005).

[5] R. S. Jacobsen, K. N. Andersen, P. I. Borel, J. Page-Pedersen, L. H. Frandsen, O. Hansen, M. Kristensen, A. V. Lavrinenko, G. Moulin, H. Ou, C. Peucheret, B. Zsidri, and A. Bjarklev, “Strained silicon as a new electro-optical material,” *Nature* **441**, 199-202 (2006).

[6] Jonathan E. Roth , Onur Fidaner , Rebecca K. Schaevitz , Yu-Hsuan Kuo , Theodore I. Kamins, James S. Harris, Jr. , and David A. B. Miller, “Optical modulator on silicon employing germanium quantum wells,” *Opt. Express* **15**, 5851-5859 (2007).

[7] A. W. Fang, H. Park, O. Cohen, R. Jones, M. J. Paniccia, and J. E. Bowers, "Electrically pumped hybrid AlGaInAs-silicon evanescent laser," *Opt. Express* **14**, 9203-9210 (2006).

[8] Hyundai Park, Ying-hao Kuo, Alexander W. Fang, Richard Jones, Oded Cohen, Mario J. Paniccia, and John E. Bowers, “A hybrid AlGaInAs-silicon evanescent preamplifier and photodetector,” *Opt. Express* **15**, Issue 21, 13539-13546 (2007).

[9] J. Raring, E. Skogen, L. Johansson, M. N. Sysak, J. Barton, M. L. Mašanović, L. Coldren, "Demonstration of Widely-Tunable Single-Chip 10 Gb/s Laser-Modulators Using Multiple-Bandgap InGaAsP Quantum-Well Intermixing," *IEEE Photon. Technol. Lett.*, **16**, 1613-1615 (2004).

[10] J. Shimizu, M. Aoki, T.Tsuchiya, M. Shirai,A. Taike, T. Ohtoshi, and S. Tsuji, “Advantages of optical modulators with InGaAlAs / InGaAlAs MQW structure,” *Electron. Lett.*, **38**, 821–822 (2002).

[11] Hideki Fukano, Takayuki Yamanaka, Munehisa Tamura, and Yasuhiro Kondo, “Very-Low-Driving-Voltage Electroabsorption Modulators Operating at 40Gb/s,” *IEEE J. Lightwave Techno.* **24**, 2219-2224 (2006).

[12] K. Kato, A. Kozen, Y. Muramoto, Y. Itaya, T. Nagatsuma, and M.Yaita, "110-GHz, 50%-efficiency mushroom-mesa waveguide p-i-n photodiode for a 1.55-μm wavelength,” *IEEE Photon. Technol. Lett.*, **6**,719–721 (1994).